

## MIT Open Access Articles

*Integration of vertically-aligned carbon nanotube forests in microfluidic devices for multiscale isolation of bioparticles*

The MIT Faculty has made this article openly available. **Please share** how this access benefits you. Your story matters.

**Citation:** Fachin, F. et al. "Integration of vertically-aligned carbon nanotube forests in microfluidic devices for multiscale isolation of bioparticles." 2010 IEEE SENSORS. 47-51. ©2010 IEEE.

**As Published:** <http://dx.doi.org/10.1109/ICSENS.2010.5690852>

**Publisher:** Institute of Electrical and Electronics Engineers

**Persistent URL:** <http://hdl.handle.net/1721.1/65845>

**Version:** Final published version: final published article, as it appeared in a journal, conference proceedings, or other formally published context

**Terms of Use:** Article is made available in accordance with the publisher's policy and may be subject to US copyright law. Please refer to the publisher's site for terms of use.



# Integration of Vertically-Aligned Carbon Nanotube Forests in Microfluidic Devices for Multiscale Isolation of Bioparticles

F. Fachin, B. L. Wardle  
Dept. of Aeronautics and Astronautics  
Massachusetts Institute of Technology  
Cambridge, MA 02139  
ffachin@mit.edu, wardle@mit.edu

G. D. Chen, M. Toner  
BioMEMS Resource Center  
Massachusetts General Hospital  
Charlestown, MA 02129  
gracec@mit.edu, mehmet\_toner@hms.harvard.edu

**Abstract**—Presently, an estimated 35 million people are living with HIV, 300 million with Hepatitis C (HCV), with thousands of human fatalities registered ever day due to these and similar infectious diseases. Efficient, reliable, inexpensive medical solutions are therefore needed to tackle these issues. Identification of HIV and HCV is however not easy. Being significantly smaller than cells and bacteria, these viruses escape the isolation capabilities of both macroscopic and microscopic (MEMS) medical instrumentation. Allowing access to sub-micron species such as viruses and cancer cells, integration of nanotechnologies in medical devices has the potential to revolutionize the field of biomedicine. In this work, we explore the potential of nanoporous, patterned forests of vertically-aligned carbon nanotubes (VACNTs) for bioparticle isolation, demonstrating their ability to access particles over several orders of magnitude in size, from viruses ( $\sim 40\text{nm}$ ) to cells ( $\sim 10\mu\text{m}$ ). Modifying the flow field inside microfluidic channels, CNT-enhanced biodevices result in a seven-fold increase in capture efficiency compared to a nonporous design, as well as the ability to simultaneously isolate multiple distinct biospecies both inside and on the outer surface of the VACNT features. Our technology represents a versatile, highly efficient approach to biological isolation, with applications ranging from point-of-care diagnostics to subsequent therapeutic modalities in both infectious diseases as well as cancer applications.

## I. INTRODUCTION

During the last decade microsystems have begun to play a major role in a variety of biomedical fields, from molecular/cell biology (e.g., flow cytometry/sorting), to point-of-care devices (e.g., immunosensors) [1]. Having dimensions on the order of micrometers, MEMS features allow manipulation of biological particles that macroscopic instrumentation cannot easily access (e.g., bacteria and cells; Fig. 1). Yet, some of the current, most widely spread diseases are associated with smaller, sub-micron bioparticles, such as viruses and exosomes, that intrinsically escape the capabilities of microdevices. For instance, both the human immunodeficiency virus (HIV) and the hepatitis C virus (HCV) range between 50 to 100 nm in size, thus being beyond the isolation possibilities of MEMS devices. Integration of nanotechnologies into biomedical systems is therefore attractive, as it could enable devices and applications capable of targeting both sub- and super-micron species (Fig. 1), targeting a much

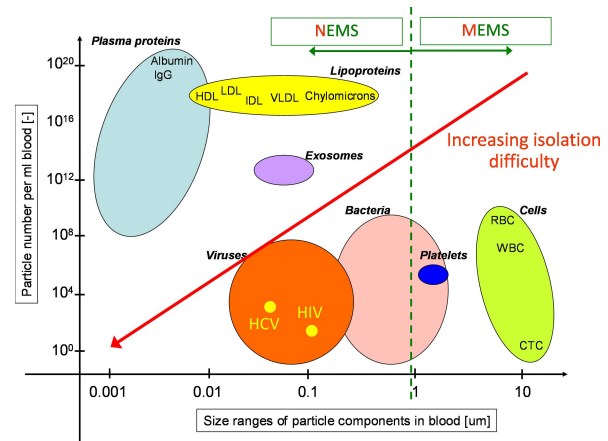


Fig. 1. Bioparticle quantity and size in blood. Carbon nanotube-based biodevices (NEMS) could allow access to particles that current microsystems (MEMS) cannot manipulate.

larger variety of diseases. In this work, we investigate the potential of nanoporous carbon nanotube (CNTs) arrays in biomedicine. Dispersed, randomly-oriented CNTs have already been adopted in a number of biomedical applications, from biological imaging techniques (optical tags) to electrical label-free bio-species detection [2]. The findings by Kam et al. [3] and Pantarotto et al. [4] suggesting that functionalized CNTs can freely enter cells by themselves without toxicity have fostered research into the use of CNTs in biomedicine, ultimately leading to applications such as CNT-mediated delivery of small drugs and bio-macromolecules [5] and *in vivo* tumor targeting using carbon nanotubes [6]. However, prior approaches to CNT-based biomedical devices do not take advantage of the physical properties of carbon nanotube forests (e.g., tailorability, aspect ratio, porosity), thus being limited solely to chemical CNT-biospecies interactions. Furthermore, being based on very specific chemical functionalization of dispersed CNTs, these methods are incapable of providing a general platform for simultaneous isolation, detection and manipulation of multiple biological species on a single chip.

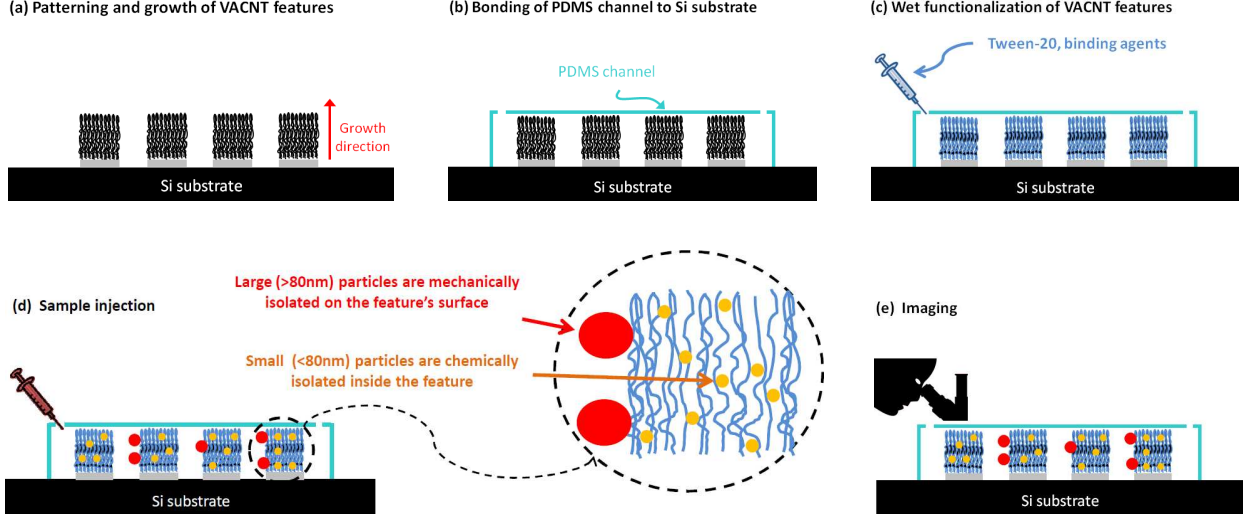


Fig. 2. Multiscale bioparticle isolation using micro-patterned VACNT features in microfluidic channels: schematics of fabrication, functionalization and bio-identification. Not to scale.

To overcome these limitations, we explore the potential of patterned, functionalized, nanoporous microfeatures of VACNTs in biomedicine, demonstrating that their physical properties allow for simultaneous mechanical and chemical multiscale bioparticle isolation. Patterned forests of VACNTs are incorporated into microfluidic devices and functionalized using wet chemistry, resulting in ultra-high porosity (99%) features for isolation of bioparticles over three orders of magnitude in size. Showing the highest capture efficiency recorded, the nanoporous features have the potential to enable applications such as virus depletion/concentration and exosome isolation for cancer monitoring.

## II. METHODS

### A. Patterning, growth, and microfluidic integration of VACNT forests

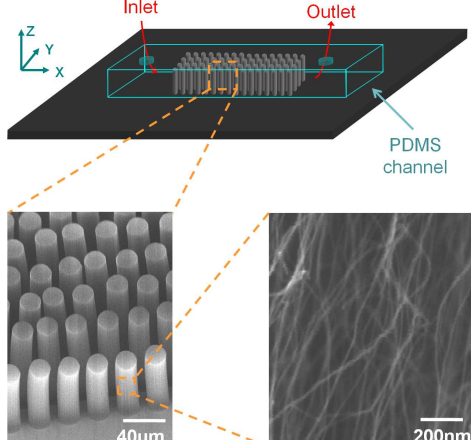
The fabrication process utilized in this work is schematically presented in Figures 2(a)-2(e). Standard photolithography is used to pattern plain  $<100>$  152mm (6") silicon wafers, followed by electron beam deposition of a 10nm  $\text{Al}_2\text{O}_3$  layer and a 1nm Fe layer. Catalyst areas are then defined by photoresist lift-off, soaking the wafer in acetone for 10 minutes with mild sonification. CNT growth is performed in a 102mm (4") quartz tube chemical vapor deposition (CVD) furnace at atmospheric pressure using reactant gases of  $\text{C}_2\text{H}_4$ ,  $\text{H}_2$  and He (400/400/1900 sccm). Catalyst annealing is carried out in a reducing  $\text{He}/\text{H}_2$  environment at  $680^\circ\text{C}$ , leading to the formation of iron (Fe) catalyst nanoparticles  $\sim 10\text{nm}$  in diameter.  $\text{C}_2\text{H}_4$  is then introduced into the furnace to initiate CNT growth, occurring at a rate of approximately  $100\mu\text{m}/\text{min}$  until the flow of  $\text{C}_2\text{H}_4$  is discontinued. The technique results in forests of multi-walled (2-3 concentric walls), vertically-aligned carbon nanotubes, with an average tube diameter of

8nm and an average inter-CNT spacing of  $\sim 80\text{nm}$ , giving a 1% volume fraction (Figure 2(a) and insets in Figure 3(a)) [7].

Incorporation of the patterned CNT structures into devices is achieved using standard soft lithography techniques. Polydimethylsiloxane (PDMS) caps ( $2\text{cm} \times 3\text{mm} \times 100\mu\text{m}$ ) are fabricated from SU-8 photoresist negative molds, and bonded to the silicon wafers containing the CNT features after oxygen plasma treatment. Microfluidic channels are created via holes at either side of the PDMS caps, thus allowing for the possibility to inject biosamples into the channel that interact with the nanoporous features (Figure 2(b)). In Figure 3 we present both a schematic representation and a device example of a patterned VACNT feature (rectangular array of  $20\mu\text{m}$  diameter cylindrical pillar features) integrated in a microfluidic device. The vertical-alignment of the nanotubes in the forest is noticeable in the insets of Figure 3(a).

### B. Forest functionalization using wet chemistry

The devices are functionalized based on the method proposed by Chen et al. in [8]. First, 1,1 carbonyldiimidazole (CDI) is reacted with Tween 20 for 2 hours at  $40^\circ\text{C}$ , resulting in CDI-activated Tween. Pressure-driven injection of a solution of CDI-activated Tween (1 wt%, water) into the microchannel (Fig. 2(c)) is then used to functionalize the micropatterned CNT features, followed by flushing using DI water. This non-covalent functionalization yields a monolayer of Tween molecules bound to the VACNTs, thus suppressing non-specific binding (NSB) of proteins such as human IgG and BSA [8]. A second functionalization step is then performed to enable selective biological recognition of target species. A solution containing avidin in buffer is injected into the channels, resulting in a covalent link between the avidin and the Tween-activated nanotubes. For the experiment on capturing model viral particles, the avidin-coated CNTs were



(a) Schematic of a nanoengineered biodevice for bioparticle isolation. Insets show SEMs of patterned VACNT forests.



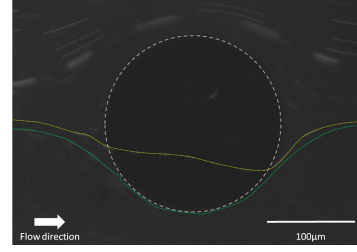
(b) Example of patterned, nanoporous CNT forest integrated in a microfluidic device.

Fig. 3. Example of nanoengineered biomedical device for multiscale bioparticle isolation using VACNT features.

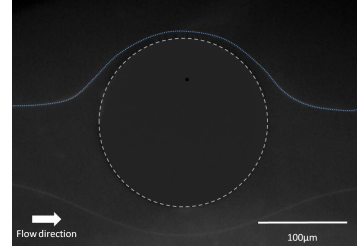
used directly to bind biotin-coated nanoparticles. For experiments on *Escherichia coli* bacteria capture, a biotinylated anti-*Escherichia coli* antibody was injected after the avidin step. Noticeably, although all the functionalization methods in this work are based on wet chemistry, no post-growth forest treatment is required to ensure that the forests' structural properties are maintained: even after wetting, the CNT features preserve their geometry.

### C. Bioparticle injection and imaging

Particle isolation is achieved through pressure-driven injection of biosamples in the microchannel and through the nanoporous features (flow rate:  $10 \mu\text{L}/\text{min}$ , Fig. 2(d)). Selective species recognition is obtained both via chemical affinity/attraction and by mechanical manipulation of particles based on their physical properties, as described in Section III. Final imaging is performed using either a fluorescent or a confocal microscope (Fig. 2(e)). No additional CNT treatment is required to ensure the integrity of the features under operation. Even during sample flow, the features maintain their geometry without bending, an ability perhaps associated with



(a) Quantum dots (20nm in diameter) touch (bottom, green streamline) and penetrate (middle, yellow streamline) the nanoporous CNT features.



(b) Quantum dots (20nm in diameter) do not reach the solid PDMS surface (top, blue streamline) due to boundary layer effects.

Fig. 4. Flow of quantum dots around two cylindrical (a) CNT and (b) PDMS pillars: streamline images relative to a 10 seconds interval (acquisition frequency: 1 frame/second).

the ultra-high porosity characterizing our VACNT forests (see Section III).

## III. RESULTS

As discussed in Section II-A, the features in this work are composed of vertically-aligned carbon nanotubes forests, with an average tube diameter of approximately 8nm, an average inter-CNT spacing of about 80nm, and 1% CNT volume fraction. Our nanoporous features are therefore highly porous, with 99% of the overall structural volume being void and only 1% being solid. Integrating nanoporous elements into microfluidic channels, our technology modifies boundary layer effects, one of the main obstacles in bioparticle separation using chemical affinity/attraction. This results in a flow field where streamlines often contact the surface of the CNT features (bottom, green streamline in Fig. 4(a)), thus greatly increasing capture probability. Furthermore, nanoporosity results in the possibility for small particles - i.e. particles smaller than the average inter-CNT spacing ( $\sim 80\text{nm}$ ) - to penetrate the forest (middle, yellow streamline in 4(a)), thus providing additional interaction between the targets and the features. This is in contrast with traditional designs that make use of solid materials such as PDMS and silicon for the features, where capture efficiency is greatly limited by the presence of a structural boundary layer surrounding the impermeable features that impedes particles to reach the features' surfaces (top, blue streamline in Fig. 4(b)). Nanoporosity also results in a drastic increase in surface area

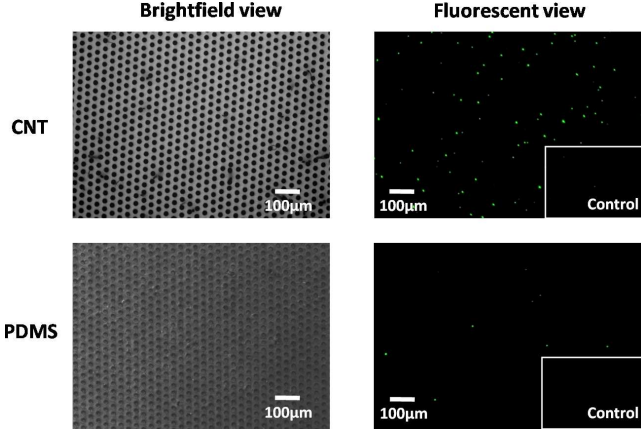
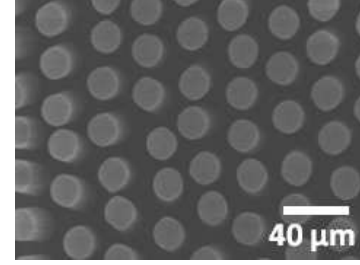


Fig. 5. Isolation of *Escherichia coli* bacteria ( $\sim 1\mu\text{m}$ , green particles in fluorescent view) using functionalized VACNT and PDMS micropillar features. Results show a seven-fold increase in capture efficiency when nanoporous CNT structures are utilized.

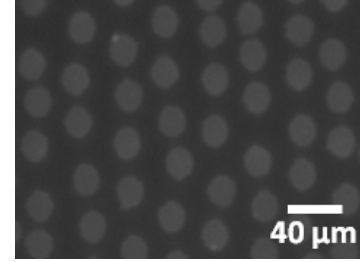
compared to solid designs ( $\sim 600\times$  for a  $100\mu\text{m}$  diameter PDMS cylindrical post vs. a  $100\mu\text{m}$  diameter nanoporous cylindrical post feature), further enhancing the isolation capability of our devices. The effect of nanoporosity on capture efficiency is evident in Figure 5, where we compare microfluidic isolation of *Escherichia coli* bacteria using two identically shaped ( $30\mu\text{m}$  diameter pillars) VACNT and PDMS structures. Relative to the solid PDMS design, the nanoporous features show a seven-fold increase in capture efficiency.

Forest nanoporosity also results in the possibility to isolate biological species ranging several orders in size, from viruses and exosomes ( $\sim 10\text{-}100\text{nm}$ ) to bacteria and cells ( $\sim 1\text{-}10\mu\text{m}$ ), using a single chip. Particles smaller than the average inter-CNT spacing ( $\sim 80\text{nm}$ ) that penetrate the features, can be isolated inside the nanoporous features, while larger particles can be captured on the features' external surface. As an example, in Figure 6 we present the results of two different bioassays performed using functionalized, patterned forests of  $20\mu\text{m}$  cylindrical VACNT pillar features (Fig. 6(a)). Here, particles ranging more than two orders of magnitude in size are captured using chemical and mechanical means:  $40\text{nm}$  virus-like beads, whose size is smaller than the average inter-CNT spacing of  $80\text{nm}$ , are trapped inside the pillars (Fig. 6(b)), while larger  $1\mu\text{m}$  bacteria-like beads are isolated on the external surface of the pillars (Fig. 6(c)).

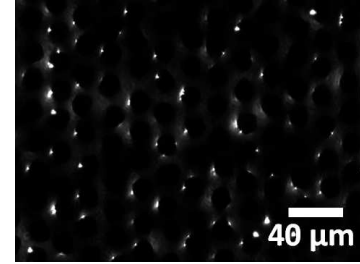
Next to chemical affinity-based isolation, nanoporous CNT features allow for different mechanical bioparticle captures as well. If used as "filters", CNT features enable mechanical isolation of bioparticles based primarily on particle size relative to inter-CNT spacing: while particles smaller than the average inter-CNT spacing ( $\sim 80\text{nm}$ ) penetrate the forest, larger particles (such as cells) are unable to cross the CNT feature boundaries, thus being mechanically filtered. This capture strategy is presented in Figure 7, where we use rectangularly shaped forests ( $500\mu\text{m} \times 200\mu\text{m} \times$



(a) SEM of an "as-grown" array of cylindrical VACNT pillar features



(b)  $40\text{nm}$  virus-like beads are captured inside the VACNT pillar features.



(c)  $1\mu\text{m}$  bacteria-like beads accumulate on the pillar features' external surfaces.

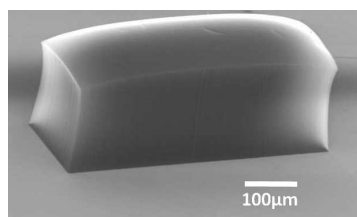
Fig. 6. Mechanical/chemical bioparticle isolation using nanoporous pillar features.

$100\mu\text{m}$ ) to mechanically isolate non-functionalized  $1\mu\text{m}$  (green) beads (Fig. 7(b)). Combining the above chemical and mechanical capture strategies, simultaneous multiscale bioparticle isolation via nanoporous CNT features can also be achieved. This is demonstrated in Figure 7(c), where we use functionalized CNT "filters" to simultaneously isolate  $1\mu\text{m}$  non-functionalized beads (green) as well as  $50\text{nm}$  avidin-coated beads (red). While the  $1\mu\text{m}$  beads are mechanically trapped on the front surface of the CNT feature, the  $50\text{nm}$  avidin-coated beads are trapped inside the forest due to their chemical interaction with the functionalized CNT surfaces.

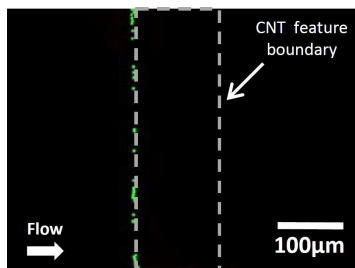
#### IV. CONCLUSIONS AND PERSPECTIVES

Experimental research was carried out to demonstrate micropatterned, nanoporous carbon nanotubes features in microfluidic devices for multiscale isolation and manipulation of biological species. We demonstrated that transitioning from solid to nanoporous microfluidic design results both in a

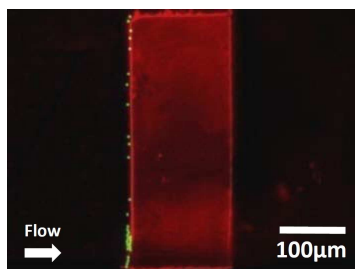




(a) SEM of an “as-grown” rectangular VACNT forest.



(b)  $1\mu\text{m}$  non-functionalized beads are mechanically filtered on the front edge of the CNT forest.



(c) Simultaneous isolation of  $1\mu\text{m}$  non-functionalized (green) and 50nm avidin-coated (red) beads.

Fig. 7. Simultaneous multiscale mechanical and chemical bioparticle isolation using VACNT “filter” features.

seven-fold increase in bioparticle capture efficiency, and in the possibility to perform simultaneous multiscale mechanical and chemical isolation on a single chip. The method is simple (no dedicated machinery required, other than an optical microscope) and versatile in that it allows targeting of different biospecies by controlling the functionalization strategy and/or the inter-CNT spacing (i.e., the forest porosity). Further flexibility is then provided by the possibility of tailoring the forest using standard photolithography, thus allowing for a variety of feature designs. In conclusion, our method represents a versatile approach to multiscale bioparticle isolation applicable to a number of applications, from global health diagnostics, particle depletion and desalination.

#### ACKNOWLEDGMENTS

This work was supported by the U.S. Department of State’s Fulbright Science and Technology Award, and the National Institute of Biomedical Imaging and Bioengineering under Grant P41 EB002503 (BioMEMS Resource Center).

#### REFERENCES

- [1] W. Wang and S. A. Soper, *Bio-MEMS: Technologies and Applications*. CRC Press, USA, 2006.
- [2] Z. Liu, S. Tabakman, K. Welsher, and H. Dai, “Carbon nanotubes in biology and biomedicine: *In vitro* and *in vivo* detection, imaging and drug delivery,” *Nano Research*, vol. 2, pp. 85–120, February 2009.
- [3] N. W. S. Kam, T. C. Jessop, P. A. Wender, and H. J. Dai, “Nanotube molecular transporters: Internalization of carbon nanotube-protein conjugates into mammalian cells,” *Journal of the American Chemical Society*, vol. 126, pp. 6850–6851, 2004.
- [4] D. Pantarotto, J. P. Briand, M. Prato, and A. Bianco, “Translocation of bioactive peptides across cell membranes by carbon nanotubes,” *Chemical Communications*, pp. 16–17, 2004.
- [5] N. W. S. Kam, Z. A. Liu, and H. J. Dai, “Carbon nanotubes as intracellular transporters for proteins and DNA: An investigation of the uptake mechanism and pathway,” *Angewandte Chemie International Edition*, vol. 45, pp. 577–581, 2006.
- [6] Z. Liu, K. Chen., C. Davis, S. Sherlock, Q. Cao, X. Chen, and H. Dai, “Drug delivery with carbon nanotubes for *in vivo* cancer treatment,” *Cancer Research*, vol. 68, pp. 6652–6660, 2008.
- [7] B. L. Wardle, D. S. Saito, E. J. García, A. J. Hart, R. G. de Villoria, and E. A. Verploegen, “Fabrication and characterization of ultrahigh-volume-fraction aligned carbon nanotube-polymer composites,” *Advanced Materials*, vol. 20, pp. 2070–2714, 2008.
- [8] R. J. Chen, S. Bangsaruntip, K. A. Drouvalakis, N. W. S. Kam, M. Shim, Y. Li, W. Kim, P. J. Utz., and H. Dai, “Noncovalent functionalization of carbon nanotubes for highly specific electronic biosensors,” *PNAS*, vol. 100, pp. 4984–4989, April 29 2003.